Detection of changes in playa development with satellite data & GIS

MAHDI SAGHAFI[1] & MAHIN RASTEGAR MOGHADDAM[2]

[1] Tabriz University. (e-mail: msaghafi@Tabrizu.ac.ir)
[2] Educational Organization. (e-mail: Marastegar@Yahoo.com)

Abstract: The development of playas caused by natural or human-induced processes is a major environmental hazard. Playas are one of the main saline environments. The global extent of primary salt-affected soils is about 955 M ha, while secondary salinization affects some 77 M ha, with 58% of these in irrigated areas. This requires careful monitoring of the soil salinity status and variation to curb degradation trends, and secure sustainable land use and management.

Remote sensing facilitates cross-scale validation, enables analysis of processes and patterns in time and space, and is thus viable for the conduct of earth system science. Multi-temporal optical and microwave remote sensing can significantly contribute to detecting temporal changes of salt-related surface features. This paper reviews various sources such as: aerial photographs, satellite- and video imagery and approaches used for remote identification and mapping of salt-affected areas. Constraints on the use of remote sensing data for mapping salt affected areas are shown related to the spectral behaviours of salt types, spatial distribution of salts on the terrain surface, temporal changes on salinity, interference of vegetation, and spectral confusions with other terrain surfaces.

Kahak playa is located in the south of Birjand city, Iran. Remote sensing data need substantial transformation for proper feature recognition and mapping. In this paper techniques such as spectral un-mixing, maximum likelihood classification, fuzzy classification, band rationing, principal components analysis, and correlation equations are discussed. Lastly, the paper presents modelling of temporal and spatial changes of salinity and playa-developing using combined approaches that incorporate different data fusion and data integration techniques.

Résumé: Le développement des playas provoqués par des processus normaux ou humain-induits est un danger pour l'environnement important. Playas sont l'un des environnements salins principaux. L'ampleur globale des sols sel-affectés primaires est environ 955 M ha, alors que le salinization secondaire en affecte 77 M ha, avec 58% de ces derniers dans des secteurs irrigués. Ceci exige de la surveillance soigneuse du statut et de la variation de salinité de sol pour limiter des tendances de dégradation, et pour fixer l'utilisation et la gestion de la terre soutenables.

La télédétection facilite croix-mesurent la validation, permettent l'analyse des processus et des modèles à temps et l'espace, et sont ainsi viable pour la conduite de la science de système de la terre. La télédétection multi-temporelle optique et de micro-onde peut de manière significative contribuer à détecter les changements temporels des dispositifs extérieurs sel-connexes. Cet article passe en revue de diverses sources comme : photographies, satellite aérien et langage figuré et approches de vidéo utilisés pour l'identification et tracer à distance des secteurs sel-affectés. Des contraintes sur l'utilisation des données de télédétection pour des secteurs affectés par sel traçants sont montrées connexes aux comportements spectraux des types de sel, à la distribution spatiale des sels sur la surface de terrain, aux changements temporels sur la salinité, à l'interférence de la végétation, et aux confusions spectrales avec d'autres surfaces de terrain.

Le playa de Kahak est situé dans les sud de la ville de Birjand, Iran. Les données de télédétection ont besoin de la transformation substantielle pour l'identification et tracer appropriés de dispositif. En cela des techniques de papier telles que la classification spectrale de maximum de vraisemblance un-se mélangeant et, la classification brouillée, l'analyse de composants rationnants et principaux de bande, et les équations de corrélation sont discutées. Pour finir, modeler de présents de papier des changements temporels et spatiaux de la salinité et playa-développement en utilisant les approches combinées qui incorporent la différentes fusion de données et techniques d'intégration de données.

Keywords: Remote sensing, geomorphology, materials, land use

INTRODUCTION

Playas, or terminal lakes are closed depressions with minimal topographic relief, common in most semi and arid-environments typical of desert areas, (Figure 1). Their origin may be related to the individual or combined intervention of a wide variety of processes, including aeolian erosion (Cooke et al. 1993; Goudie 1991, Goudie and Wells 1995). Other processes thought to form shallow (1–3m depth) closed basin playas are tectonic origin (Sinha-Roy, 1986, Roy, 1999), excessive late Pleistocene siltation at river confluences (Ghosh, 1964; Ghosh et al., 1977) and formation of sand dunes across river channels. The physical and chemical evolutions of these playas are attributed to favourable geomorphologic, tectonic and climatic conditions. These playas are economically very important as some thousands of tons of salts are produced every year from their brine.

These geomorphic features have different names, depending upon the culture that dominates the region of their occurrence. The terms ‘playa’ or ‘playa lake’ are often confused or inappropriately used, or have been replaced by a somewhat synonymous term at a specific locale, such as ‘dry lake’ that is used in California (Briere, 2000; Rosen,

1994). Thus, we find sabkhas (inland and coastal) and its variant spellings in the Arabic-speaking world; salinas, salares, saladas, salars, and playas in many Spanish-speaking cultures; pans, saline lakes, alkali flats, salt plains, dry lakes, and salt flats in English-speaking cultures. Rosen (1994) provides useful information regarding the terminology of these saline environments in different areas of the earth. Perusal of the Glossary of Geology (Bates and Jackson 1987) provides nearly 40 names for these features. However, to hydrogeologists, they represent a single hydrogeologic process with varying elevation of ground water relative to the surface, and different boundary and initial conditions. Both ground and surface waters can accumulate within a terminal basin and result in flooding of the playa.

One of the problems in monitoring and preserving these playa-lakes is the scarcity of records about their hydrologic conditions and associated environments with ecological meaning. Only some temporary and unpublished ground records are available, but remotely sensed data can surrogate ground observations if spectral or other features of the satellite image allow reliable interpretation. Corroborating ground data, even over a limited time span, can increase the satellite information evidential value, facilitating the detection of key factors that condition environmental preservation such as agriculture and irrigation. The literature does show an increasing interest in characterizing and monitoring wetlands by remote sensing (Zhang et al., 1997; Lunetta and Balogh, 1999; Frazier and Page, 2000; Houhoulis and Michener, 2000; Munyati, 2000; Chopra et al., 2001).

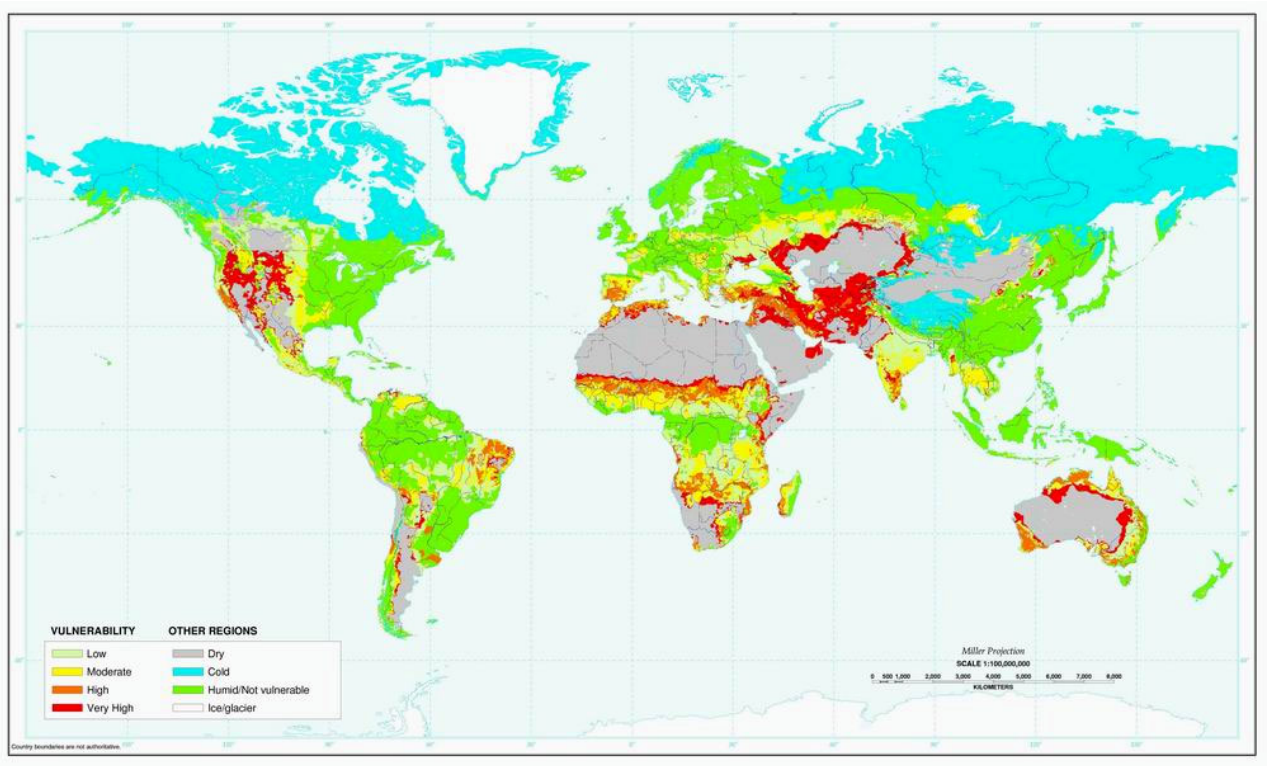

Figure 1. Location of desertification vulnerable area in the world (US Department of Agriculture Natural Resources Conservation Service, Washington DC 1998).

Vulnerable ecosystems associated with playa are often faced with land use transformation and with changes in the aquifers usually connected to them. Many articles studied have investigated humid and vegetated wetlands threatened by desiccation, and located both in coastal and flood plain environments (Al Saifi and Qary, 1996; Kasishke and Bourgeau-Chavez, 1997; Dwivedi et al., 1999; Rao et al., 1999; Baghdadi et al., 2001). Frequently, these researches aim to detect and delineate the water bodies and estimate their change. For this purpose, some of them have used Landsat imagery, taking advantage of the analysis potential stemming from its spatial and temporal resolution, and the continuity of the image acquisition that began in 1972. Verdin (1996) discriminated ephemeral water bodies of between 1 and 150 ha in Nigeria. Drake and Bryant (1994) monitored the flooding ratio of Tunisian playas-lakes sized from 90 to 5500 km2 for study the climatic changes on the playas hydrology. Bryant and Rainey (2002) examined the response of these playas to seasonal changes, and identified inundation process stages within the saline pan by changes in the surface reflectance properties of the playa-lake bed. Changes in the water extent of playas and closed salt lakes have been estimated by remote sensing to Asses changes in regional climate (Schneider et al. 1985; Harris, 1994; Bryant, 1999; Birkett, 2000). Nakayama et al. (1997) detected changes in the water area and volume of Central Asian lakes and related them to environmental parameters. Remote sensing may provide a temporal perspective of the playa-lakes hydrology in the absence of historical data such as water levels (Al-Khudhairy et al., 2002).

GEOGRAPHICAL AND GEOLOGICAL SETTING

The site chosen for this study is a salt playa south of Birjand, south Khorasan province, Iran. The playa named Kahak and is situated between the Bagheran Mountains in the North and east and Khonik mountains in the south and west. The study area was located in 32°23′ - 32°39′ E and 59°01′ - 59°34′ N (Figure 2). The area has a cold arid climate. Rainfall displays high inter-annual and seasonal variability, annual precipitation of study area is 150 mm. From May to September, the natural drying process of playa takes place and only sporadic inflow of water occurs as a result of slight rains. The mean maximum temperature in the region ranges between 20 and 43 C. The playa area is up to 17 Km^2, and the catchment area of the basin is 2500 km^2.

Gaz River, which is one of the sub basins of Birjand Salt River drainage basin, is the only integrated drainage network flowing from the Mokhtaran plain and confluence with Birjand Salt River in to the Lute desert. The presence of a number of palaeo-channels throughout the desert suggests the existence of a former fluvial system in the region. Poor drainage has led to the accumulation of the rainwater in the various large and small natural depressions (playas), which later became saline during a period of higher evaporation in the region. Due to the relatively higher precipitation, seasonal rivers and streams feed the playas. During the months that precipitation occurred (cold seasons), these streams carry detritus and dissolved solids into the playas. The level of soil salinity is related to the balance between the deposition of salt through evaporation and the dilution effect of precipitation.

The Kahak playa is located within the wind gaps between the Bagheran Mountains at an altitude of 2720 m above the m.s.l and Khonik Mountains at an altitude of 2503 m above the m.s.l. It is the most extensive and economically most important playa of the region. The playa is elongated in NW–SE direction, 43 km in length and 1-3 km in width and altitude of it is about 1490 m above means sea level (Figure 2).

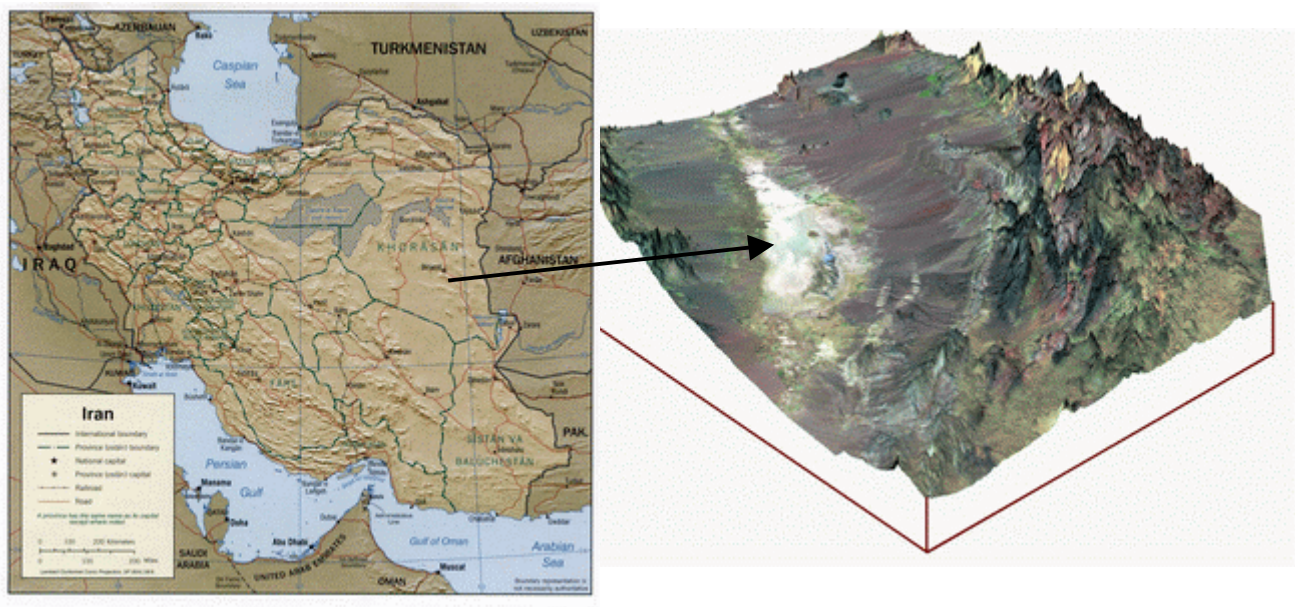

Figure 2. The study area.

Geological and geochemical observations in the region indicate the presence of metamorphic rocks of varying petrographic character, intrusions of pegmatites and volcanics. Rocks of several groups belonging to the Cretaceous and Tertiary constitute the Bagheran mountain system (Figure 3). The Cretaceous groups include: Peridotite (Harzburgite-Lherzolite), Coloured Mélange, and Shale-Sandstone in the north and north east of area, and The Tertiary groups include of Tuff-Marl-Conglomerate in the south and south west of the study area (Table 1). Widespread volcanic event at the end of the Mesozoic is marked by the isolated exposures of the Bagheran igneous suite. This igneous suite consisting of basalt and rhyolite.

Several landforms and sacrificial deposits are identified in the area including stepped sequences of fluvial terraces, Aeolian accumulations, debris-covered slopes, talus flatirons, blowouts and playas. Some of these landforms and deposits record changes in the surface processes induced by climatic variations in Quaternary times.

Table 1. Geological characteristics of the study area.

ROCK TYPE	**LITHOLOGY**	**ERA**	**PERIOD**	**EPOC**	**FACI**	**AREA (Km2)**
IGNEOUS	PERIDOTITE (HARZBURGITE-LHERZOLITE)	MESOZOIC	CRETACEOUS	UPPER	PLUTONIC	140
METAMORPHIC	COLOURED MELANGE	MESOZOIC	CRETACEOUS	UPPER	DISLOCATION METAMORPHISM	49
SEDIMENTARY	SHALE-SANDSTONE	MESOZOIC	CRETACEOUS	UPPER	DETRITAL	996
VOLCANOSEDIMENTARY	TUFF-MARL-CONGLOMERATE	CENOZOIC	TERTIARY	OLIGO/MIOCENE	PYROCLASTIC	122

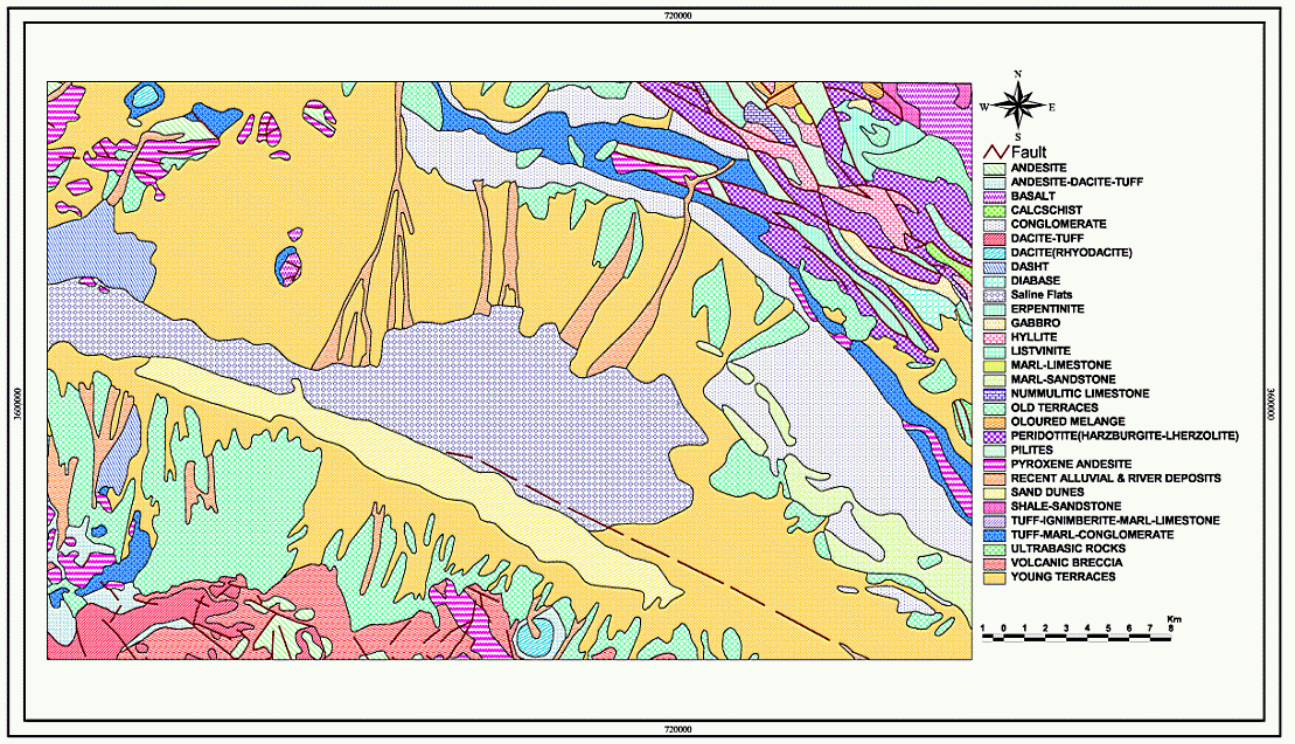

Figure 3. Geological map of the study area.

METHODOLOGY

This study uses 2 Landsat TM and ETM+ images spanning 14 years from 1988 and 2002. Both them represent the summer seasons because they were acquired for this specific study. Table 2 show the dates of these images and their specifications.

Table 2. Specifications of used images

Instrument	Resolution	Date	Scene ID	Satellite
TM10	28.5	September 1988	2231036-01 WRS =159/03700	Landsat 4
ETM+	28.5	September 2002	2231036-01 WRS =159/03700	Landsat 5

First, the satellite images were corrected. After checking the uniformity of the atmosphere over the scenes, a simple haze compensation procedure (Richards and Jia, 1999) was applied to minimize the influence of path radiance effects (Lillesand and Kieffer, 2000). Then, a subscene of 1200 km^2 containing the study area was extracted and registered. Co-registration of all images is necessary in order to analyses the change detection of playa in the study area. To establish co-registration of all images, control points from the Iranian Army Topographic maps at 1:25000 scales were used as a reference for the 1988 image and the other images were registered to this subscene. Approximately 27 ground-control points were selected from topographic-map features that could be identified on each image. An independent set of points was selected and used to assess the accuracy of the co-registration. The root-mean-square error (rms) of verification points is a better estimator of registration accuracy, than the rms of the control points used for developing the rectification model (Dwyer, 1995). The maximum verification error from co-registration of all

images was 53 m in the X- and 67 m in the Y-direction. All images were resampled to form a pixel size of 25 m. After registration, topographic maps and aerial photographs were used to generate a slope map.

We considered areas with less than 2 degree slope as plains with Kahak playa located in the centre of it that were analysed further in this study. We then extracted information from images to identify surface characteristics and their associated facies. Five methods were applied to extract information from satellite images: (1) Visual analysis and supervised classification. The outlines of the salty area (visually identified from with RGB values of 741) were combined with supervised classification from two period images and extracted using Maximum Likelihood (ML) Classification. Pixels are assigned to pre-selected classes based on a decision rule, which maximizes the likelihood of having obtained the observed values given the overall assignment of classes to the image. (2) Principal components analysis change detection, (3) Material mapping indexes such as: Bicarbonate Calcium, Halite, Ilit, Kaolinite, Montmorillonite and Sodium (ERDAS Field Guide, 2002), (4) Tasseled cap transformation and (5) Texture analysis of the PCA. These methods were selected as the most commonly used for temporal comparisons. Several factors such as tone, texture and location were considered for every band. In order to enhance the spectral signatures of the playa-lake covers, the IHS transformation (Liu and Moore, 1990; Lillesand and Kieffer, 2000) of the images was applied at the 432 and 457 compositions. Also, the principal component analysis was applied over the six original bands taking advantage of the information compression and image enhancement properties of this transformation (Richards and Jia, 1999).

Urbanized, undisturbed, and agricultural regions of the study area give rise to different texture. These different types of landuse have distinct spatial edge frequencies or texture that can be used as input in to classification algorithms (Gong&Howarth, 1990). Urban areas typically have significant texture resulting from building sand street grids, whereas homogeneous areas such as agricultural fields have little ton texture. Texture values were calculated from the PCA1 images. Principal component (PC) images were prepared for the all-remote sensing images. The first three PC images (PC 1, 2, 3) contained 97% of the variation of the original six TM bands, which is a significant compression of data. The first PC image (PC 1) is a weighted positive sum of all the original bands and it represents a panchromatic view of the area containing 88% of the data variance. It was dominated by topography, expressed as highlights and shadows that are highly correlated in all six of the original TM bands.

We then calculated detection of changes. In this study we used all available methods inlcuding: principle components analysis (PCA), change vector analysis (CVA) (Singh (1989), multi-date classification and differencing of derived indexes

Finally eight base maps and indices (Bicarbonate Calcium, Halite, Ilite, Kaolinite, Montmorillonite, Sodium, Tasseled cap transformation and Texture analysis of the PCA) were created with this imagery and each was used as a training image in the models. These were used in the fuzzy classification method for determination area with critical changes. Fuzzy classification produced a series of images where the membership of each pixel is determined based on spectral similarity to training sites and user confidence of homogeneity of training sites (z score).

RESULT AND DISCUSSION

The spectrally corrected images were classified using a supervised classification approach with a maximum likelihood classifier (Campbell, 1996). Separate sets of training areas were collected for the 1988 imagery and the 2002 imagery. Because of the wide range of digital values belonging to each class, salt class that could be easily recognized in the field was used for the purpose of the classification. Training data for this study were selected by sampling the area covered by each class. Training data sets for the salt class were constructed separately for each of the seven-bands. To improve the validity of the statistical estimates, Swain and Davis (1978) recommended that the training areas should include a minimum of 10*N* pixels, and if possible 100*N* pixels, *N* being the number of image channels used in the classification. In this case, between 9422*N* and 12173*N* pixels were randomly selected using on-screen sampling of independent pixels distributed over the entire images (Table 3). All training areas were collected with the seed pixel method (Lillesand and Kiefer, 1994). The spectral signatures used for the classification process were generated by pooling the training data from all seven bands because the spectral corrections were highly successful in removing differences in brightness among the images.

The outlined salty area numbered 500-600, with sizes ranging from 400m^2 to 8 Km^2. The resultant images displaying only the playa-lakes and salty depressions are referred to as target images (Figure 4). With comparison of the areal extent of the salty area in the playa lake between 1988 and 2002 images, we find that about 626878 m2 increased to the areal extent of salty area of the 1988 year (Table 4)

Table 3. Characteristics of training area for classification of salt area from two periods images (In pixel).

1988						2002				
Band	**Mean**	**StDev**	**Nr**	**Pred**	**Total**	**Mean**	**StDev**	**Nr**	**Pred**	**Total**
1	254.9	0.9	11919	255	12173	254.5	1.9	8740	255	9422
2	255	0.5	12111	255	12173	255	0.3	9381	255	9422
3	254.9	0.6	12061	255	12173	255	0.3	9363	255	9422
4	254.9	0.7	12041	255	12173	254.6	1.2	8424	255	9422
5	254.9	1	11861	255	12173	253	3.6	6444	255	9422
6	97.6	13.2	2832	112	12173	170.8	9.2	2636	176	9422
7	254.9	0.8	12029	255	12173	253.6	3.1	7441	255	9422

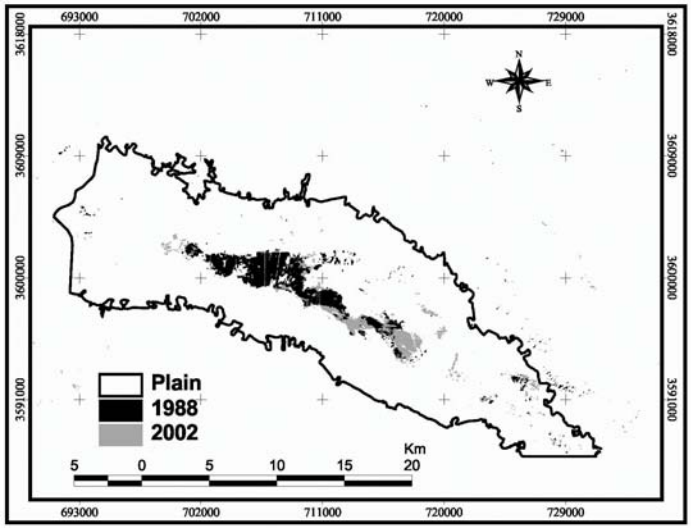

Figure 4. Salty are in the 1988 and 2002 year

Table 4. Changes in the two period of the areal extent of the playa (In m2)(Figure.3).

	1988	**2002**	**Common**	**Changes**
Sum	17356800	16729925	7552162.5	626875
Mean	33637.209	27247.435	18419.909	6389.774
Maximum	7481200	8171262.5	1728350	-690062.5
Minimum	400	400	50	0
Variance	183469000000	124135000000	18463198220	59333648207
Standard Deviation	428332.54	352328.138	135879.352	76004.402

A characteristic of PCA is that information common to all input bands (high correlation bands) is mapped to the first Principal Component (PC) image (the one with the largest eigenvalue). Subsequent PCs (those with smaller eigenvalues) account for progressively less of the total scene variance. We can apply this principal to multi-temporal datasets. If two images covering the same ground area but taken at different times of the year (at the same wavelength) are subjected to PCA, then the first PC image will contain all of the information that has not changed between the two dates, in other words, that part of the data that is highly correlated (i. e. most similar) between the two input images. The second PC image will contain all the change information, that is, that part of the data that is less correlated (i. e. less similar) between the two input images (Table 5 and Figure 5). If we load the second PC, the areas of greatest change between the two input images are found in the tails of its histogram (Figure 6).

Table 5. Eigenstructure of the Principal Component Analysis of two period images.

Variance per band: 23069.24, 3715.64, 2545.61, 1124.64, 664.91, 506.20, 177.46, 101.91, 69.09, 51.47, 30.82, 25.49, 20.15, 14.57 Variance percentages per band: 71.83, 11.57, 7.93, 3.50, 2.07, 1.58, 0.55, 0.32, 0.22, 0.16, 0.10, 0.08, 0.06, 0.05														
	Image 1988							Image 2002						
	Tmb1	**Tmb2**	**Tmb3**	**Tmb4**	**Tmb5**	**Tmb6**	**Tmb7**	**Tmb1**	**Tmb2**	**Tmb3**	**Tmb4**	**Tmb5**	**Tmb6**	**Tmb7**
PC 1	0.244	0.258	0.272	0.279	0.278	0.064	0.284	0.282	0.302	0.304	0.304	0.308	0.138	0.302
PC 2	0.111	0.085	0.065	0.043	0.056	0.616	0.068	-0.059	-0.118	-0.14	-0.224	-0.171	0.678	-0.103
PC 3	-0.265	-0.283	-0.289	-0.307	-0.286	-0.05	-0.262	0.239	0.231	0.253	0.123	0.219	0.468	0.249
PC 4	0.155	0.12	0.11	0.116	0.006	-0.771	0.049	-0.035	-0.075	-0.07	-0.058	-0.194	0.52	-0.127
PC 5	-0.311	-0.19	-0.103	0.053	0.309	-0.041	0.221	-0.523	-0.308	-0.183	0.364	0.349	0.166	0.156
PC 6	0.017	0.015	0.063	0.143	-0.224	0.125	-0.195	-0.061	0.052	0.078	0.768	-0.274	0.042	-0.439
PC 7	0.271	0.2	0.234	0.21	-0.52	0.028	-0.404	-0.308	-0.215	-0.058	-0.028	0.306	-0.004	0.338
PC 8	-0.494	-0.156	0.23	0.504	-0.025	0.011	-0.055	-0.203	0.053	0.521	-0.264	-0.186	0.008	-0.004
PC 9	-0.062	-0.155	0.018	0.079	-0.327	0.019	0.41	0.162	-0.161	-0.173	0.174	-0.513	-0.046	0.559
PC 10	0.196	0.185	-0.018	-0.491	-0.174	0.007	0.357	-0.51	0.1	0.493	-0.016	-0.122	-0.01	0.001
PC 11	-0.549	0.771	-0.011	-0.145	0.019	-0.007	-0.106	0.005	0.108	-0.174	0.05	-0.105	0.011	0.127
PC 12	-0.231	0.05	0.122	0.055	-0.509	-0.003	0.515	0.208	-0.089	-0.086	-0.082	0.419	0.012	-0.4
PC 13	-0.011	0.155	-0.025	-0.139	0.123	0.005	-0.085	0.337	-0.796	0.426	0.068	0.004	-0.012	-0.017
PC 14	0.149	0.228	-0.829	0.447	-0.095	0.01	0.106	-0.048	0	0.11	-0.047	0.011	-0.011	-0.019

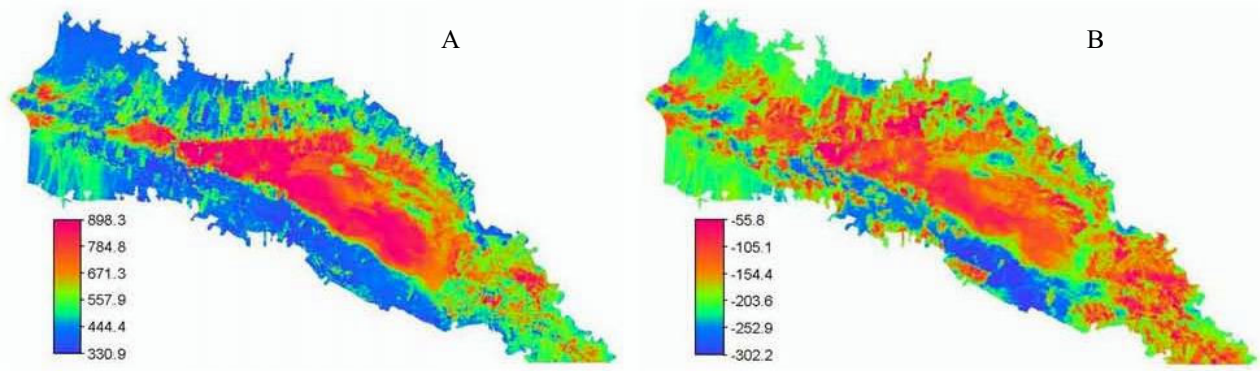

Figure 5. A. PC1 image contain all of the information that has not changed between the two dates and B. PC2 image contain all the change information.

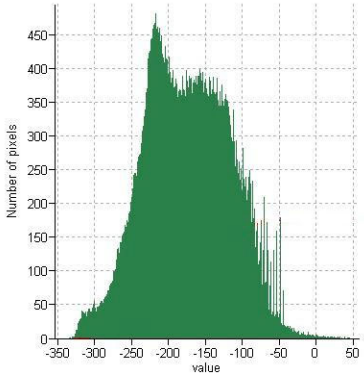

Figure 6. Histogram of PC2 image, the areas of greatest change between the two input images are found in the tails of it.

In this study the content of chemical elements: bicarbonate calcium, halite, illite, kaolinite, montmorillonite and sodium were with aim of satellite data for two period calculated for each epoch. By mapping of this material for two periods, we prepared change maps of those by image differencing method of change detection (Figure 7)

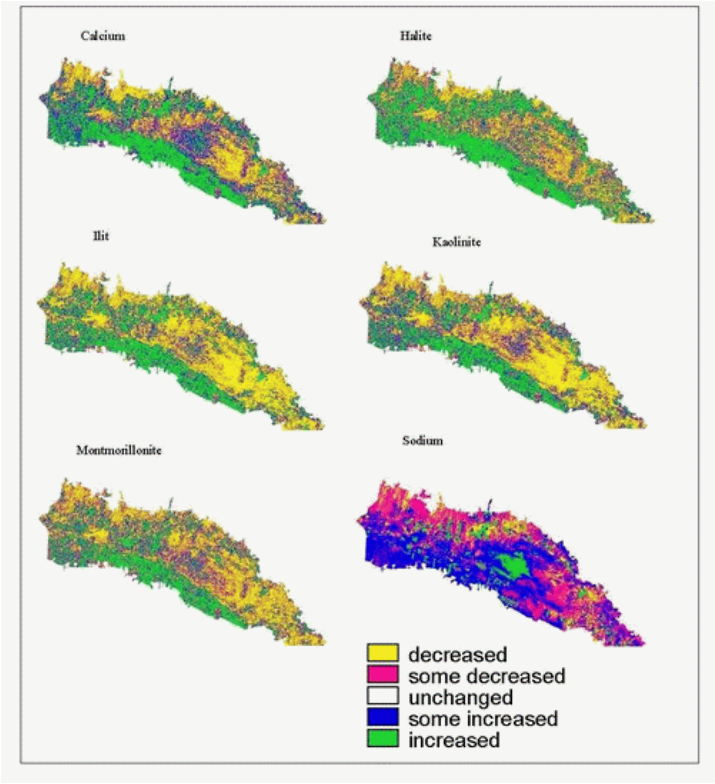

Figure 7. Changes in the chemical elements that calculated for the study area from two period mages.

To determine changes between chemical element maps of two periods, we considered of 10 percent rate to the classification of area in the five classes. Thus, we classified areas with 10 percent of increased changes as increased areas, and areas with 5 percent of increased changes as areas of some increase, and areas with 10 percent decrease as decreased areas, and areas with 5 percent decrease as areas with some decrease (Figure 8). In the study area most of the increased changes were related to the chemical elements of Halite and most decreased changes are related to illite. Thus, we find that declined rates for the area that contain illite in the 14 years and increased rates for area that contain Halite (Figure 8). To classify areas with critical changes, six change maps were overlain, and fuzzy set theory used to calculate the critical rate of change (Figure 9).

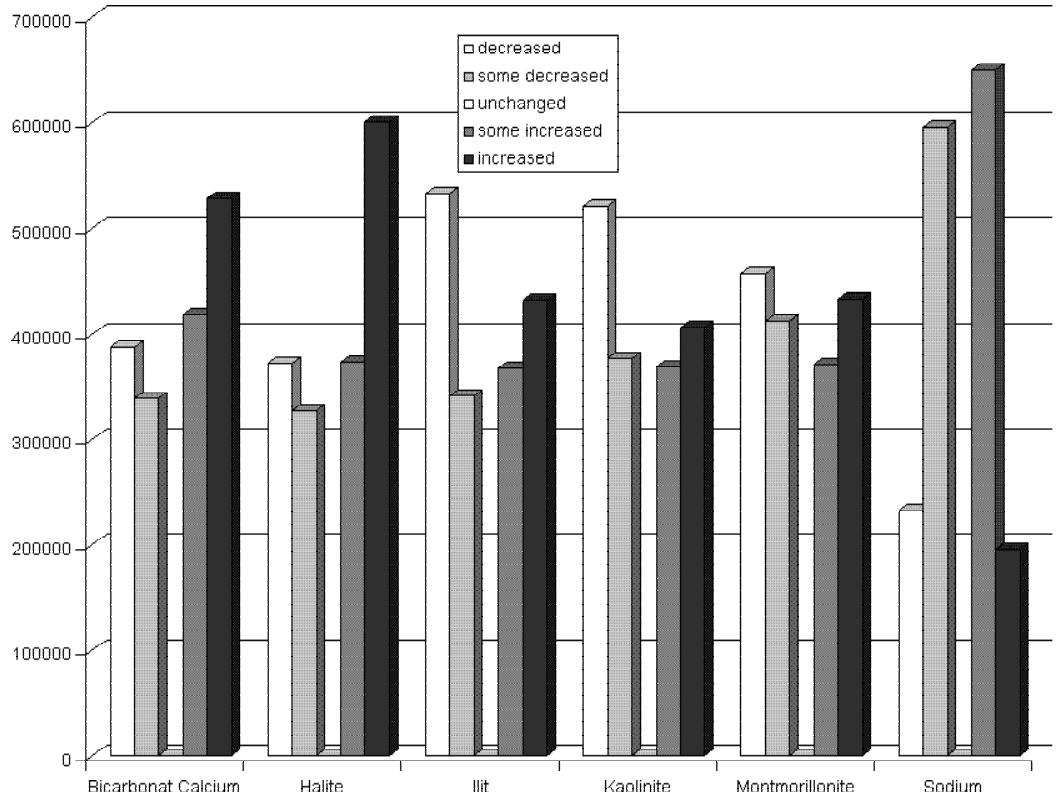

Figure 8. Rate of changes in the chemical element for the 14 years (In pixel).

This model contains six fuzzy sets with $A_1, A_2, A_3, ...A_6$ indices, and $A_1 \bigcap A_2 \bigcap A_3, ...\bigcap A_6$ membership functions by $\mu_{A_i}(x)$ is as follow:

$$\mu_{\bigcap A_i}(x)(1 \le i \le 6) = \mu_{A_1}(x) \wedge \mu_{A_2}(x) \wedge \mu_{A^3}(x) ..... \wedge \mu_{A^6}(x)$$

and

$$\mu_{A_i}(x) \wedge \mu_{A_i}(x)(1 \le i, j \le 6) = \begin{cases} \mu_{A_i}(x) & \mu_{A_i}(x) \le \mu_{A_j}(x) \\ \mu_{A_j}(x) & \mu_{A_j}(x) > \mu_{A_j}(x) \end{cases}$$

then

$$\bigcap A_i (1 \le i \le 6) = \min\{\mu_{A_1}(x), \mu_{A_2}(x) ....., \mu_{A_6}(x)$$

Classification that shown in the figure 9, considered as fallow:

Decreased if $\mu_{A_i}(x) \quad (1 \le i \le 6) \in [0, 0.25]$

Increased if $\mu_{A_i}(x) \quad (1 \le i \le 6) \in [0.75, 1]$

Some decreased if $\mu_{A_i}(x) \quad (1 \le i \le 6) \in [0.25, 0.5]$

Some increased if $\mu_{A_i}(x) \quad (1 \le i \le 6) \in [0.5, 0.75]$

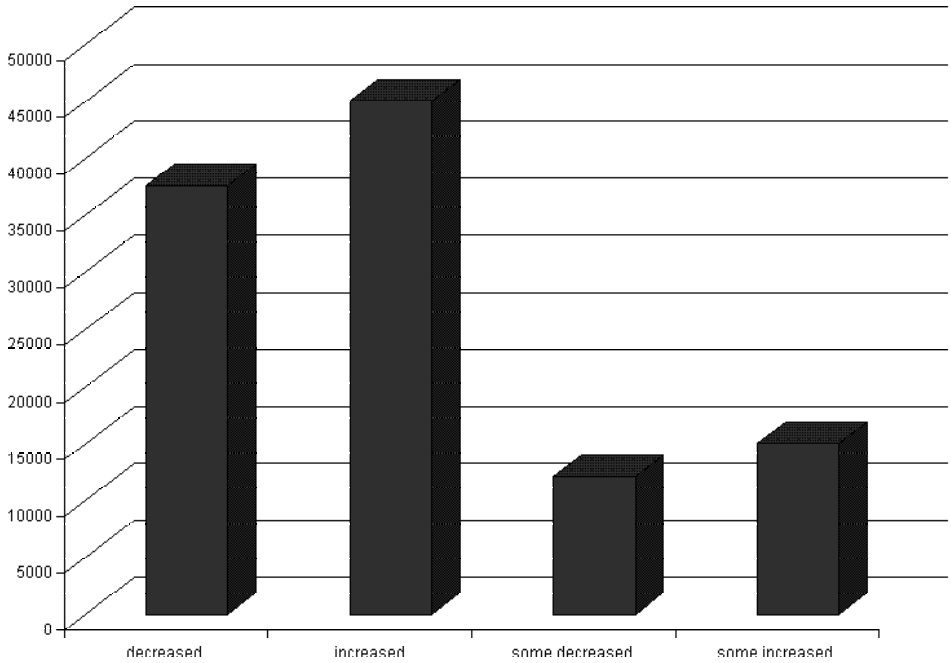

Figure 9. Result of fuzzy classification and area of the each memberships (In pixel).

Playas are wetland areas. In this study, we determined changes in the extent of wetland by computation of a tasseled cap transformation. The Tasseled cap transformation of Landsat TM has a wetness feature that contrasts the visible and NIR bands (TM1–4) with the MIR bands (TM5 and 7). The Tasseled cap transformation is a method of rotating satellite data such that the majority of the information is contained in components or features that relate directly to physical scene characteristics (Lillesand & Kiefer, 1994). The first and second features of TM are brightness and greenness, respectively. The third feature is termed wetness because it is sensitive to soil and plant moisture. In this study with aim of tasseled cap transformation, wetness of the images for two periods is calculated, and their changes determined.

An image texture analysis was used to detect variation in pattern structure as imaged in the PCA1 data. On the other hand, changes in the chemical properties of the playa lake result in morphological and micro relief variations. To detect this we used texture analysis and determined the variety of texture for two period PCA1 images and calculate differences between them (Table 6).

Finally, a correlation matrix between eight maps such as: bicarbonate calcium, halite, illite, kaolinite, montmorillonite, sodium, Tasseled cap and Texture was calculated. Results show that relationships between chemical changes are strong. But between other chemical elements, changes in the rate of sodium more correlated with changes in the texture and pattern of the playa with correlation value about of 0.11(Table 6).

Table 6 Correlation matrix between eight changes map.

Mean per band: 0.06, 0.06, -0.00, -0.00, -0.00, 0.02, 1.72, 61.58 Std. per band: 0.26, 0.22, 0.07, 0.08, 0.03, 0.12, 54.4, 597.96								
Indexes	**Bicarbonate Calcium**	**Halite**	**Ilit**	**Kaolinite**	**Montmorillonite**	**Sodium**	**Tasseled cap**	**Texture**
Bicarbonate Calcium	1	0.92	0.95	0.95	0.86	0.4	-0.06	0.08
Halite	0.92	1	0.92	0.86	0.91	0.01	-0.21	0.04
Ilit	0.95	0.92	1	0.98	0.96	0.25	-0.12	0.05
Kaolinite	0.95	0.86	0.98	1	0.91	0.38	-0.06	0.08
Montmorillonite	0.86	0.91	0.96	0.91	1	0.08	-0.17	0.01
Sodium	0.4	0.01	0.25	0.38	0.08	1	0.38	0.11
Tasselcp	-0.06	-0.21	-0.12	-0.06	-0.17	0.38	1	0.02
Texture	0.08	0.04	0.05	0.08	0.01	0.11	0.02	1

CONCLUSION

There are several digital change detection algorithms or techniques, which have been developed and used over the years to estimate changes using remote sensing (in most cases satellite) data. These techniques are based on various mathematical and/or statistical relationships, principles and assumptions. The use of one specific change detection

technique or method over another can calculate a significantly different estimate of the change for a same area. Therefore, it is important to use the most appropriate technique to study a particular area and environment.

An overall aim of this study was to detect and map changes in the areal extent of playa over time, several standard, commonly used image-analysis techniques were considered. This project successfully shows that change detection techniques can be applied to playa environments. Analysis of the change data provides information to assess landscape level changes in vegetation extent and composition. It also affords information on causal agents that are having the greatest impact throughout a project area. The change data also benefits existing programs. Incorporating change data with field observation of area enhances the ability to correctly map changes in vegetation extent and composition. Research is required to define thresholds between change classes representing quantitative changes in canopy reduction and growth. Although the numbers representing acres of detected change have not been verified by an accuracy assessment, correlations do exist between detected change and other factors such as: bicarbonate calcium, halite, illite, kaolinite, montmorillonite and sodium, development and regeneration. Accuracy assessment procedures are being implemented into future project areas. Verified data may provide input to the sustainable planning and management of cities.

Acknowledgements: Thank you to Dr. M.H. REZAEI MOGHADDAM of the University of Tabriz for review of this paper and helps, and Birjand Agricultural Organization for their assistance in obtaining materials.

Corresponding author: Dr Mahdi Saghafi, Tabriz University, 29th Bahman, Tabriz, East Azerbaijan, P.O.Box 51665 - 145, Iran. Tel: 0098-411-3392272. Email: msaghafi@Tabrizu.ac.ir.

REFERENCES

AL SAIFI, M.M. & QARY, M.Y.H.T. 1996. Application of Landsat Thematic Mapper data in sabkha studies at the Red Sea coast. *International Journal of Remote Sensing*, **17** (3), 527–536.

AL-KHUDHAIRY, D.H.A., LEEMHUIS, C., HOFFMANN, V., SHEPHERD, I.M., CALAON, R., THOMPSON, J.R., GAVIN, H., GASCA-TUCKER, D.L., ZALIDIS, G., BILAS, G. & PAPADIMOS, D. 2002. Monitoring wetland ditch water levels using Landsat TM and ground-based measurements. *Photogrammetric Engineering and Remote Sensing*, **68** (8), 809–818.

BAGHDADI, N., BERNIER, M., GAUTIER, R. & NEESON, I. 2001. Evaluation of C-band SAR data for wetlands mapping. *International Journal of Remote Sensing*, **22** (1), 71–88.

BATES, R.L. & JACKSON, J.A., 1987. *Glossary of geology*. American Geological Institute, USA.

BIRKETT C.M. 2000. Synergistic remote sensing of Lake Chad: inundation, *Remote Sensing of the Environment*, **72**, (2) 218-236.

BRIERE, P.R. 2000. Playa, playa lake, Sabkha: proposed definitions for old terms. *Journal of Arid Environments*, **45**, 1–7.

BRYANT, R.G. & RAINEY, M.P. 2002. Investigation of flood inundation on playas within the zone of Chotts, using a time-series of AVHRR. *Remote Sensing of the Environment*, **82**, 360–375.

BRYANT, R.G. 1999. Application of AVHRR to monitoring a climatically sensitive playa. Case study: Chott El Djerid, Southern Tunisia. *Earth Surface Processes and Landforms*, **24**, 283–302.

CAMPBELL, J. B. 1996. *Introduction to remote sensing*, 2nd ed. Taylor and Francis, London.

CHOPRA, R., VERMA, V.K. & SHARMA, P.K. 2001. Mapping, monitoring and conservation of Harike wetland ecosystem, Punjab, India, through remote sensing. *International Journal of Remote Sensing*, **22** (1), 89–98.

COOKE, R.V., WARREN, A. & GOUDIE, A.S., 1993. *Desert geomorphology*. UCL Press, London. 526 p.

DRAKE, N.A. & BRYANT, R.G. 1994. Monitoring the flood ratio of Tunisian playas using Advanced Very High Resolution Radiometer (AVHRR) imagery. *In: Millington, A.C., Pye, K. (Eds.), Environmental Change in Drylands: Biogeographical and Geomorphological Perspectives*. Wiley, New York, pp. 347–364.

DWIVEDI, R.S., RAO, B.R.M. & BHATTACHARYA, S. 1999. Mapping wetlands of the Sundaban Delta and its environs using ERS-1 SAR data. *International Journal of Remote Sensing,* **20** (11), 2235–2247.

DWYER, J. L. 1995. Mapping tidewater glacier dynamics in East Greenland using Landsat data, **41**(139): 584–595.

ERDAS. 2002, ERDAS Field Guide, 6rd ed., ERDAS, Inc, Atlanta, GA, 686 pp.

FRAZIER, P.S. & PAGE, K.J. 2000. Water body detection and delineation with Landsat TM data. *Photogrammetric Engineering and Remote Sensing*, **66** (12), 1461–1467.

GHOSH, B. 1964. Geomorphological aspects of the formation of salt basins in western Rajasthan. *In: Proceedings of the Symposium on Problems of Indian Arid Zone. Ministry of Education, Government of India and UNESCO, CAZRI, Jodhpur*, 79–83.

GHOSH, B., SINGH, S. & KAR, A. 1977. Desertification around the Thar—a geomorphological interpretation. *Ann. Arid Zone*, **16**, 290–301.

GONG, P. & HOWARTH, P.J. 1990. Theuseofstructuralinformationforimprovingland-over classification accuracies at the rural–urbanfringe. *PhotogrammetricEngineeringandRemoteSensing*, **56**(1), 67–73.

GOUDIE, A.S. & WELLS, G.L. 1995. The nature, distribution and formation of pans in arid zones. *Earth-Science Reviews*, **38**, 1 – 69.

GOUDIE, A.S. 1991. Pans. *Progress in Physical Geography*, **15** (3), 221–237.

Harris, A.R., 1994. Time series remote sensing of a climatically sensitive lake. *Remote Sensing of Environment* 50, 83–94.

HOUHOULIS, P.F. & MICHENER, W.K. 2000. Detecting wetland change: a rule-based approach using NWI and SPOT-XS data. *Photogrammetric Engineering and Remote Sensing*, **66** (2), 205–211.

KASISHKE, E.S. & BOURGEAU-CHAVEZ, L.L. 1997. Monitoring South Florida wetlands using ERS-1 SAR imagery. *Photogrammetric Engineering and Remote Sensing*, **63** (3), 281–291.

LILLESAND, T.M. & KIEFFER, R.W. 2000. *Remote sensing and image interpretation*, 4th ed. Wiley, New York 724p.

LILLESAND, T. M., & KIEFER, R. W. 1994. *Remote sensing and image interpretation*, Wiley, New York.

MITSCH, W. J. & GOSSELINK, J.G. 1986. *Wetlands*, Van Nostrand Reinhold, New York.

LIU, L.G. & MOORE, J.M. 1990. Hue image RGB colour composition. A simple technique to suppress shadow and enhance spectral signature. *International Journal of Remote Sensing*, **11** (8), 1521–1530.

LUNETTA, R.S. & BALOGH, M.E. 1999. Application of multi-temporal landsat 5TM imagery for wetland identification. *Photogrammetric Engineering and Remote Sensing*, **65** (11), 1303–1310.

MUNYATI, C. 2000. Wetland change detection on the Kafue Flats, Zambia, by classification of a multitemporal remote sensing image dataset. *International Journal of Remote Sensing*, **21** (9), 1787–1806.

NAKAYAMA, Y., TANAKA, S., SUGIMURA, T. & ENDO, K. 1997. Analysis of hydrological changes in lakes of Asian arid zone by satellite data. *In: Cecchi, G., Engman, E.T., Zilioli, E. (Eds.), Earth Surface Remote Sensing, Proceedings of SPIE–The International Society for Optical Engineering*. Bellingham, Washington, **3222**, 201–210.

RAO, B.R.M., DWIVEDI, R.S., KUSHWAHA, P.S., BHATTACHARIA, S.N., ANAND, J.B. & DASGUPTA, S. 1999. Monitoring the spatial extent of coastal wetlands using ERS-1 SAR data. *International Journal of Remote Sensing,* **20** (13), 2509–2517.

RICHARDS, J.A. & JIA, X. 1999. *Remote sensing digital image analysis*, 3rd ed. Springer, Berlin 363p.

ROSEN, M.R., 1994. The importance of groundwater in playas: a review of playa classifications and the sedimentology and hydrology of playas. *In: Rosen, M.R. (Ed.), Paleoclimate and Basin Evolution of Playas Systems*, Geological Society of America, Special Paper, **189**, 2 –18.

ROY, A.B. 1999. Evolution of saline lakes in Rajasthan. *Curr. Sci*. **76**, 290–295.

SCHNEIDER, S.R., MCGINNIS JR., D.F. & STEPHENS, G. 1985. Monitoring Africa's Lake Chad basin with Landsat and NOAA satellite data. *International Journal of Remote Sensing*, **6** (1), 59–73.

SINGH, A. 1989 Digital change detection techniques using remotely-sensed data, *International Journal of Remote Sensing*, **10**, 989-1003

SINHA-ROY, S. 1986. Himalayan collision and indentation of Aravalli orogen by Bundelkhand wedge: Implications for neotectonics in Rajasthan. *In: Proceedings of the International Symposium on Neotectonics in South Asia, Dehradun, India,* 18–21.

SWAIN, P.H. & DAVIS, S. M. (Eds.). 1978, Remote sensing: the quantitative approach. McGraw-Hill, New York.

VERDIN, J.P. 1996. Remote sensing of ephemeral water bodies in western Nigeria. *International Journal of Remote Sensing*, **17** (4), 733–748.

ZHANG, M., USTIN, S.L., REJMANKOVA, E., SANDERSON, E.W. 1997. Monitoring using remote sensing. *Ecological Applications*, **7** (3), 1039–1053.